Properties of Ti-oxide thin films grown in reactive magnetron sputtering with self-heating target

R. Graillot-Vuillecot, A.-L. Thomann, T. Lecas, C. Cachoncinlle, E. Millon, A. Caillard

Properties of Ti-oxide thin films grown in reactive magnetron sputtering with self-heating target

R. Graillot-Vuillecot[1], A. L. Thomann[1], T. Lecas[1], C. Cachoncinlle[1], E. Millon[1], A. Caillard[1]

[1] Groupe de Recherches sur l'Energétique des Milieux Ionisés (GREMI), UMR7344 CNRS-Université d'Orléans, 14 rue d'Issoudun BP6744, Orléans cedex 2, France

Abstract

Titanium dioxide thin films have been synthetized by magnetron sputtering in two configurations: using a classical cooled target (cold configuration) or allowing the target temperature to rise under ion bombardment (hot target configuration). In hot configuration, the heated target emits radiations (especially infrared ones) which affect the thin film growth. The target is pure titanium sputtered in presence of argon and dioxygen gases. The crystalline quality, morphology and structure of thin films have been studied on two substrates: thermally grown SiO_2 (500 nm)/Si and c-cut sapphire. X-ray diffraction analyses revealed that anatase phase is mainly obtained in both configurations. Texture factors evidenced different main orientations: in cold target the anatase (004) peak tends to be preferred, whereas when a hot target is used, the (112) family plane is furthered. Microscopy analyses showed that the morphology changed depending on the configuration, which could be attributed to an increase of the adatom mobility at the substrate when the target is hot. Optical transmission measurements performed on titanium dioxide thin films deposited onto sapphire substrates showed that optical band gaps may be tuned depending on the configuration used during deposition.

Keywords: magnetron sputtering, hot target, titanium oxide, optical band gap, thin film

1. Introduction

Magnetron sputtering (MS) is a well-known physical vapour deposition process for synthetizing nanoparticles or thin films. Titanium oxides (TiO_2) are well documented compounds with wide applications depending on the structural phases: anatase phase exhibits interesting photocatalytic and self-cleaning properties and rutile phase is usually used for protective and optical coating [1][2][3][4][5][6]. The growth of TiO_2 films by reactive sputtering of titanium in Ar/O_2 atmosphere has been largely studied in order to optimize its properties for the required application, by varying deposition parameters such as the target to substrate distance, the deposition time, the total pressure, the oxygen percentage, the *in-operando* annealing etc. [7][8][9][10]. However, the correlation between structural and morphological properties of films and the reactive sputtering regime is not obvious whereas it must be perfectly known and predicted for industrials. For example, films obtained in different Ar/O_2 proportions have been compared although the thickness was different because of the variation of the deposition rate between elemental and poisoned mode [8]. Since the main crystalline phases may also depend on the film thickness [11], this can lead to erroneous conclusions about the relationship between films properties and deposition conditions.

One of the latest and interesting evolutions of MS involves sputtering of a target which temperature is increased and can even exceed its melting point. For this purpose, a low heat conducting material (ceramics disk/powder, vacuum channels in the copper body or at the back side of the target) is inserted between the target and the water-cooled magnetron body with or without the presence of a crucible. An alternative approach to enhance the temperature of the target material is the use of high-power discharges [12][13][14][15][16][17] eventually coupled with the pulsed injection of gas in the vicinity of the target surface (Gas Injection Magnetron Sputtering technique) [18] in order to promote its cooling and temperature stabilization. This technique has been poorly investigated for the deposition of numerous metals and few oxides with the presence of O_2 in the gas phase. Nevertheless, its interest is growing due to the enhanced deposition rate related to the combining of sublimation/evaporation processes and to an improvement of sputtering efficiency at high temperature. The synthesis of titanium thin film and its compounds (nitrides and oxides) has been explored in the past twenty years [19] especially by a research group from Wroclaw University [20][21]. This group used the so-called technique low pressure hot target reactive sputtering (LP HTRS) or high-energy reactive magnetron sputtering (HE RMS) : the energy of the species interacting with the growing film was enhanced by using very low pressure (<0.1 Pa) of pure oxygen as a working gas and a heated metallic target partially disconnected from the water-cooled magnetron body enabling

the emission of radiation especially in the IR range. Thanks to that, sputtered species approaching the substrate have enhanced kinetic and thermal energy and TiO_2-rutile could be formed (without post annealing). But, even in the hot target sputtering configuration, it seems that the film structure is difficult to predict because other authors mainly observed the formation of anatase phase when the target temperature is enhanced by its thermal disconnection [22]. A hot target has been also used in the case of TiO_2 thin films doped by lanthanides (i.e. Eu) [23], which had also a direct influence on the rutile-anatase crystalline structure and its optical properties (optical transmission and photoluminescence). Moreover, in this type of process in which almost epitaxial conditions have been introduced [24], the type of stress (compression or tension) in TiO_2 thin film highly depends on the type of substrate: nature, crystallinity and orientation…[21].

In our group, the general approach about hot target magnetron sputtering is to couple gas phase and plasma analysis with films characterization in order to study mechanisms involved in the sputtering at the target and the film growth at the substrate. In a previous paper [22], we have investigated the influence of the Ti target surface temperature rise on the thin film deposition rate, on the energy incoming onto the substrate (IR radiation and energy of the sputtered species) and we have evidenced first trends on the film properties (crystalline structure, morphology and composition) in the case of pure Ar atmosphere and Ar/O_2 one. Concerning the TiO_x (with x around 2) films obtained in Ar/O_2, the conclusions were that working in hot target configuration seems to help synthesizing a nearly-stoichiometric titanium dioxide. This is consistent with an enhancement of the crystalline state of TiO_2 anatase films characterized by crystallites randomly distributed on substrate (even if an enhancement of the (112) and (211) peaks is observed).

In the present work, we aim to go deeper than in previous papers into the knowledge of the growth mode during the deposition of pure TiO_2 film using a hot target. More precisely, we attempt to clearly state whether the increase of the target surface temperature, leading to IR emission in front of the substrate influences the growth, the nature of phases (anatase, rutile), the surface morphology and the crystallization state of TiO_x films. Contrary to [20], Ar gas was added to O_2 in the sputtering chamber and the total pressure was fixed to 1 Pa in hot and cold target (classical) configuration. An extension of the mean free path of species sputtered from the target in our hot regime is not expected, except if gas rarefaction occurs near the target due to the gas heating as it is suspected [4]. The use of hot target leading to different structural properties compared to those obtained in classical configuration, the physical properties of TiO_x films are expected to depend on the target configuration. An example is given by the

comparison of optical transmission and bandgaps of TiO_x films grown in hot-and cold-configurations. Results in terms of bandgap are compared with previous works.

2. Experimental

The experiments were performed in a 6-way cross-shaped HV deposition chamber previously described in [22]. The pressure is regulated to 1 Pa during deposition with 20 sccm Ar flow rate, whereas the O_2 one is fixed to 3 (13 % of dioxygen) sccm in cold configuration and 9 sccm (31 % of dioxygen) in hot configuration for all results presented in the following section, in order to lie in the well-known compound/oxide regime. In hot configuration, the transition between metallic and compound regime is shifted to higher oxygen flow rate [4], therefore a higher value of 9 sccm has been used in hot configuration. The Ti target without (cold target configuration) or with (hot target configuration) a MACOR® 2 inches ceramic disk is clamped on the 2 inches magnetron backing plate powered by a DC power supply. This ceramic disk thermally disconnects the target and promotes its temperature rise. However, the clamping surrounding the target ensuring the electrical connection induces a residual cooling. Most of the samples were made at DC power of 150 W, corresponding to a power density of 7.4 W cm^{-2} on the 2 inches in diameter target (20.25 cm^2). The substrates, P-doped Si (100) wafer (resistivity of 10-20 Ohm.cm) covered with a thermally grown SiO_2 (500 nm) and c-cut sapphire substrates ((001) oriented Al_2O_3), were located 45 mm away from the target.

The thin film roughness R_{RMS} (root mean square roughness) and surface morphology on SiO_2/Si substrates were investigated on a Dimension Icon atomic force microscope (Bruker) in ScanAsyst/PeakForce Tapping regime with a Scanasyst-air tip (nominal spring constant of 0.4 N/m and a nominal tip radius of 2 nm). R_{RMS} was assessed in a scanning area of 0.5 × 0.5 μm^2. Cross-sections and top-views of thin films deposited on SiO_2/Si substrates were observed by scanning electron microscopy (SEM Zeiss Supra 40) in order to evaluate the thickness and characterize the microstructure. Thin films with various thicknesses (ranging from 150 nm to 1500 nm) were deposited on both types of substrates. The thickness of TiO_x films deposited on Si wafer and SiO_2/Si substrates were determined from the cross-section SEM images.

Rutherford backscattering spectroscopy (RBS) was used to determine the composition of the TiO_x films, i.e to obtain the O/Ti ratio (x value) depending on the growth conditions. The energy of probing 4He particles was 2 MeV, and the scattering angle was fixed 165°. Due to the low RBS yield on light elements, the oxygen content of the films is determined with a 5% precision.

Their structural characterization was performed by X-ray diffraction in Bragg-Brentano geometry with a diffractometer (D8 Bruker Discover) using the Cu K_α (1.54 Å). The XRD patterns were compared to ICDD files corresponding to anatase TiO_2 (00-021-1272) and rutile TiO_2 (01-076-1934) phases. Optical properties of films deposited on c-cut sapphire substrates were investigated by measuring the optical transmission in the 200-1200 nm wavelength range with a UV-Vis spectrophotometer (Cary 60 from Agilent).

Measurement of the target temperature was performed using a bichromatic pyrometer (IGAR 6 from Lumasense Technologies Gmbh) in a configuration described in [22]. Values obtained in front of the Ti target in hot configuration, are 660°C and 1010°C (± 50°C) for 50 and 150 W, respectively in pure Ar gas. From the previous study we have learned that the target emissivity being higher in compound regime, due to the formation of an oxide at the target surface, the reached temperature values are lower [22]. Typically, at 50 W the target temperature decreases of about 50°C. The target temperature decreases to 600 ±50°C when turning from metallic to oxide mode at 50 W, whereas only 950 ±50°C is reached at 150 W. Thus, this indicates that the present study has been performed in a range of moderate target temperatures, as compared to some works reported in literature [14]. Values were largely inferior to the titanium melting temperature at 1 atm (1668°C). This has to be related to the quite low power density used here. However, even in this range, the heated target emits radiations (especially in the infrared wavelength range) that could be adsorbed at the substrate. This could lead to a rise of the growth temperature. Actually, the hot target may act as a front heating source. Various thermocouple placement configurations were tested for a suitable thermocouple construction operating in stable conditions during tens of minutes. Thermocouples (type K with upper operation limit of 1260°C) were inserted through a hole in the substrate holder in order to be in contact with the surface and the substrate rear side. The connection between the thermocouple and the surface substrate is made by a straight contact. Even if a slight thermal loss at the thermocouple/substrate junction may not be excluded, the measured values provide a realistic estimation of the substrate temperature after tens of minutes, time required to reach a steady state (near-equilibrium thermal states) and the difference observed for the two configurations are significative. Thermocouple wires were enclosed each in a separate alumina tube shielding at the back side of the target in order to avoid metal coating and incorrect temperature measurements.

Whatever the deposition conditions and the kind of substrate, the temperature was found to increase during about 15-20 min, before reaching a near-equilibrium thermal states for different discharge power values. Typical values in cold configuration lie below 150°C, in good

agreement with what has been reported by other authors in literature [7][8]. In hot configuration, the reached values lie above 220°C at 150 W. It is well-known that determining the temperature of the substrate surface is challenging. It is supposed to be higher than at the back of the substrate. For instance, Musil et al evidenced that the delta between surface and backside temperature is of the order of 100°C for glass substrates [7]. However, taking into account a thermal conductivity λ of 150 $W.m^{-1}.K^{-1}$ for silicon and disregarding the thermal contact resistance, a rough estimation based on the Fourier law gives a temperature gap ΔT between the front one T_1 and the back one T_2 of the substrate :

$$\Delta T = T_1 - T_2 = \frac{e}{\lambda S}\left(J_{rad,in} - J_{rad,out}\right) \quad (1)$$

Where e is the substrate thickness (500 µm), S its surface (1 cm^2), $J_{rad,in}$ is the thermal radiation incoming onto the substrate equal to 0.5 W [22] and $J_{rad,out}$ is the thermal radiation emitted by the substrate given by the Stefan-Boltzmann equation. This rough estimation gives a temperature gap inferior to 10°C.

3. Results and Discussion

Morphological and structural properties of films

First insight into the growth of TiO_x on SiO_2/Si substrate was obtained from SEM observations of 800 nm thick films. Since deposition rates depend on the configuration, the deposition time has been tailored. Effect of the target temperature on the erosion rate has been investigated in a previous paper [22]. Values obtained at 150 W in cold and hot configurations are 7 nm/min and 12 nm/min, respectively.

It is seen on SEM images of Figure 1 that columnar structure expected in magnetron sputtering is obtained. But the density and the grain size are clearly impacted by the deposition configuration. This is especially observed on plane views where the mean size of the sharp angular grains appears larger when a cold target is used. This could indicate an enhanced lateral growth (parallel to the substrate surface). In cold configuration, the substrate temperature increases to some extent and reaches about 150 °C. Consequently, adatom mobility is certainly limited but exist. Typically, this stands for the zone 1C of the structure zone model [11]. In such conditions, faceted columns are expected, and deposited films are polycrystalline. In hot configuration the temperature reached during deposition is higher and lies around 250°C. In this case sharp grains are visible on Figure 1, exhibiting a very fine substructure. On cross-section image the film appears denser which could be attributed to a rise of the adatom mobility.

In a previous paper [22], the influence of the target surface temperature on the energy of the sputtered atoms, the radiative energy and the total energy incoming onto the substrate has been investigated. Using mass spectrometry, we observed an increase of the sputtered Ti flux but a slight decrease of their mean energy. The main modification of the total energy transferred to the substrate turning from cold to hot configuration was the part of radiation emitted by the target. Thus, the morphology change reported in the present work is a first indication that this energy contribution has an influence on the growth.

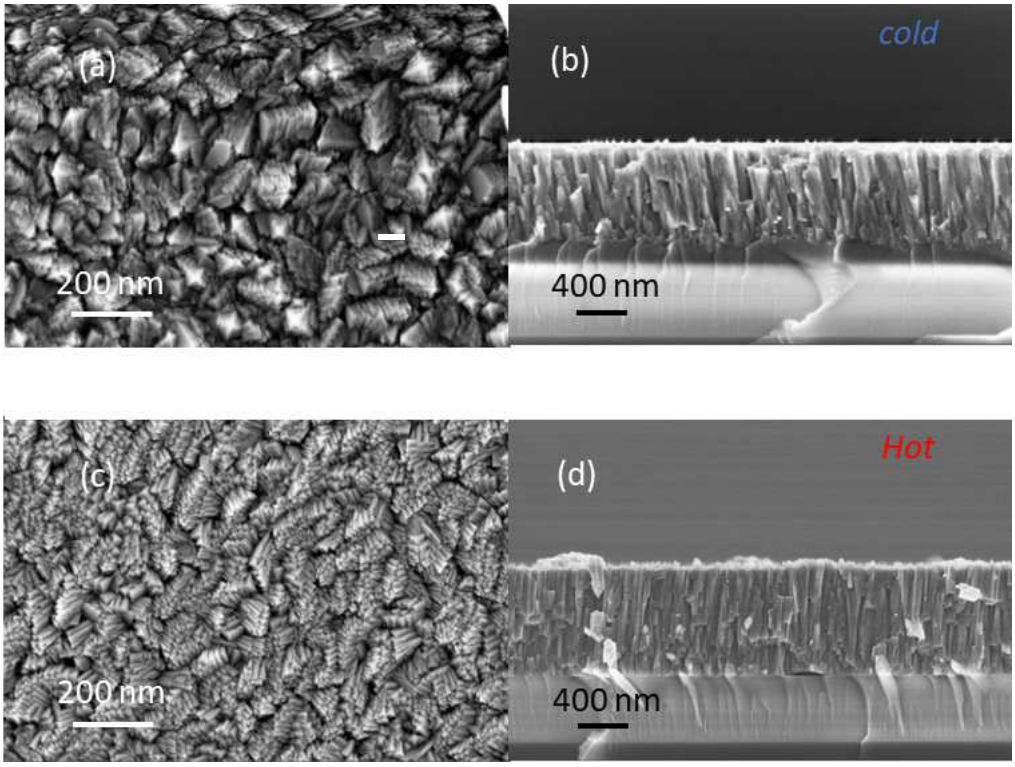

Figure 1: SEM micrographs of 800 nm thick films deposited at 150 W on SiO_2/Si substrate in cold (a,b) and hot (c,d) configurations.

To go further, AFM analysis has been performed on films deposited onto SiO_2/Si substrate. Typical images obtained in cold and hot configurations are presented Figure 2a and 2b, respectively. They are in good agreement with SEM observations. The evolution of the R_{RMS} with the film thickness is given Figure 2c. The increase of the roughness as the films become thicker is a well-known behaviour in PVD deposition [25][26]. The interesting result in Figure 2c is the slightly lower R_{RMS} value obtained in hot configuration. This trend also supports the hypothesis of an increase of the adatom mobility in this case, which competes the shadowing effect responsible for the roughness formation [11].

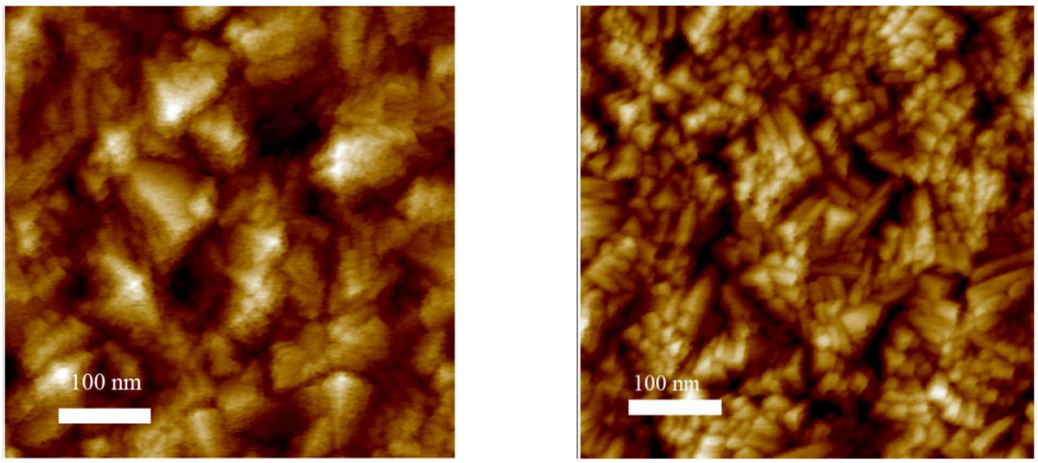

(a) (b)

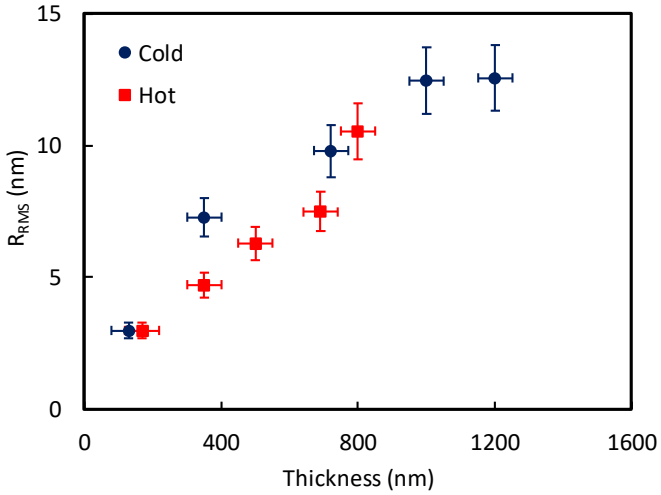

(c)

Figure 2: AFM images of films deposited onto SiO_2/Si substrate: a) 720 nm thick film in cold configuration and b) 500 nm thick film in hot configuration. c) evolution of the R_{RMS} measured on AFM images as function of the film thickness.

XRD analysis has been carried out on the films. Diffraction patterns of films of increasing thicknesses (150, 300, 700, 900 and 1200 nm) deposited in cold and hot configurations are given in Figure 3 after background subtraction. Films are found polycrystalline whatever the configuration used, and the dominant phase is anatase mixed with rutile depending on the conditions. The obtained Ti-O phases are stoichiometric (or nearly stoichiometric) since the O/Ti ratios determined by RBS measurements are found to be 2 (+/- 0.05). In addition, no other phases like titanium hydroxide are detected on the XRD diagrams.

Turning from cold to hot configuration, a change of the orientation of crystallites is observed: the intensity of (112) planes is promoted, whereas the (004) one decreases. This has already been reported in our previous work [22].

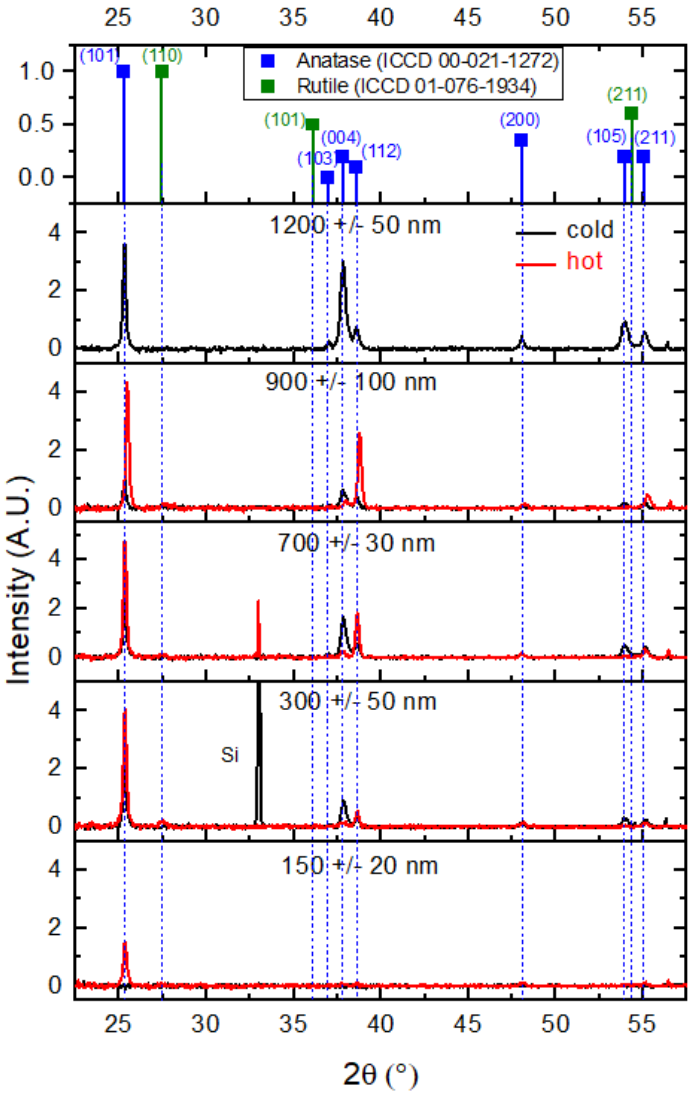

Figure 3: XRD patterns of cold (black lines) and hot (red lines) configuration for samples of different thicknesses deposited on SiO_2/Si substrates. 2θ peak position and relative intensity for anatase and rutile phases (from ICCD anatase 00-021-1272 and rutile 01-076-1934) are given on upper part of the figure.

Texture factors were calculated to get a better insight into the furthered orientations depending on the deposition configuration. Figure 4 presents the evolution of the texture factor of two crystallographic orientations of TiO_x anatase phase as function of the thickness. These texture factors were calculated using the following formula [27]:

$$p = \frac{I_{hlk\,mes}}{I_{hkl\,pow}} / \sum \frac{I_{hkl\,pow}}{I_{hkl\,mes}} \quad (1)$$

Where $I_{hkl\ mes}$ and $I_{hkl\ pow}$ stand for the measured intensity of the hkl orientation in the samples and for a randomly oriented polycrystalline sample (i.e. ICCD files), respectively.

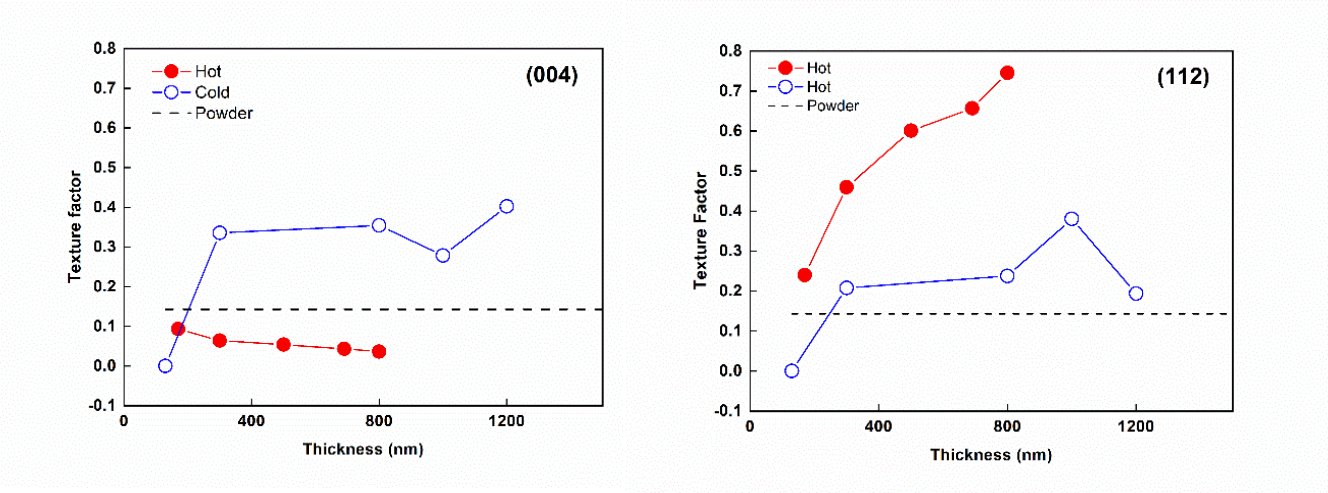

Figure 4: XRD texture factors of two family planes: (004) (left), (112) (right) calculated for anatase films with different thicknesses deposited on SiO_2/Si substrates in hot (red solid symbols) and cold (blue opened symbols) target configurations. The dotted lines correspond to the texture factors of a polycrystalline sample with randomly distributed crystallites (i.e. powder)

In cold configuration, the texture factors of each plane lie in a quite restricted range (0.1 to 0.4), whereas using a hot target clearly furthers the growth of (112) oriented planes and leads to an almost extinction of the (004) orientation. From graphs of Figure 4, it is also seen that, in cold configuration, the texture factor of all the family planes remain quite the same as the film becomes thicker. This is not the case in hot configuration, since the (112) orientation appears furthered when the thickness increases. This could be due to a continuous absorption of the IR radiation by the growing film that might result in a rise of the substrate temperature in hot configuration. Musil et al. [7], for instance, have evidenced an increase of the substrate surface temperature during the growth even after 90 min, when an oxide target, supposed to emit IR radiations, is used. We did not find such behaviour in the present work, since the temperature measured behind the substrates reaches a steady state after 15 min. Nevertheless, like for annealing process not only the reached temperature, but also the time duration may have an influence. And thick film samples have been longer exposed to the slightly higher substrate temperature. However, referring to the well-known structure zone model [11][28][29] the characteristics of these films (cross section morphology; no significant preferential orientation) indicate that in our experimental conditions we lie in the zone 1c in cold configuration. In hot configuration, the growth regime certainly enters the zone T, where preferential orientation is

observed and is related to the planes exhibiting the fastest growth kinetics. In this regime of growth, the main orientation further develops when the thickness increases [11][29].

Optical properties of films

TiO_x films have been deposited onto c-cut sapphire (Al_2O_3 (001) oriented) substrates to study their optical properties. In that way, UV-Visible optical transmission measurements have been performed. During the same runs of deposition experiment, pieces of Si wafer were placed close to sapphire substrates as references. Thicknesses of TiO_x films deposited on Si wafer were found to be 780±50 nm and 930±50 nm in cold and hot configuration, respectively. XRD analyses have been carried out on films deposited on (001) Al_2O_3 substrates. The diffractograms are given Figure 5.

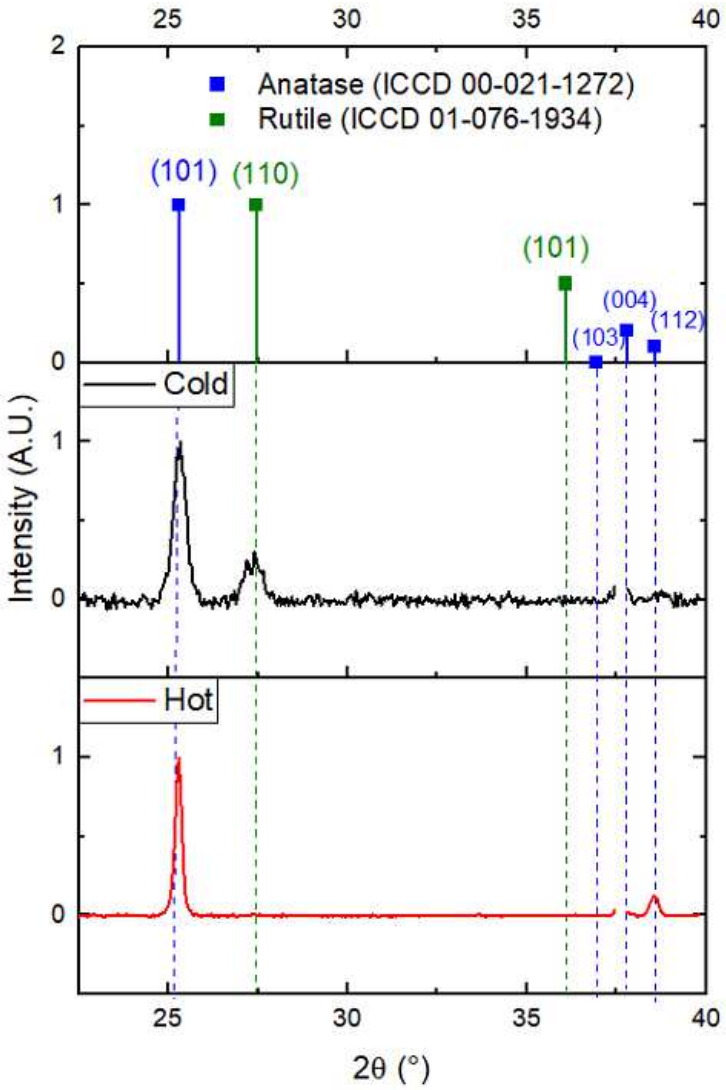

Figure 5: XRD patterns of thin films deposited on c-cut sapphire substrate in cold and hot configurations.

When turning from cold to hot configuration the same trend than evidenced on SiO_2/Si is observed: in cold configuration, the film is poorly crystallized and constituted by a mixture of anatase and rutile while only the anatase phase is formed in hot configuration. This anatase film shows a better crystallinity according to the narrowing of the peak. As observed for films deposited on SiO_2/Si substrate, an enhancement of the (112) anatase diffraction peak at $2\theta=37.8°$ is evidenced in hot configuration.

Transmission curves of TiO_2 films deposited onto sapphire are presented in Figure 6 for both hot and cold configurations. The absorption coefficient (α) of each films was deduced from :

$$\alpha = \frac{1}{t}\ln(1/T) \qquad (2)$$

where T is the transmittance and t is the film thickness, assuming the thickness of the TiO_2/c-cut sapphire films to be very close to that of the corresponding TiO_2/Si obtained from SEM cross section measurement (780±50 nm and 930±50 nm in cold and hot configuration, respectively).

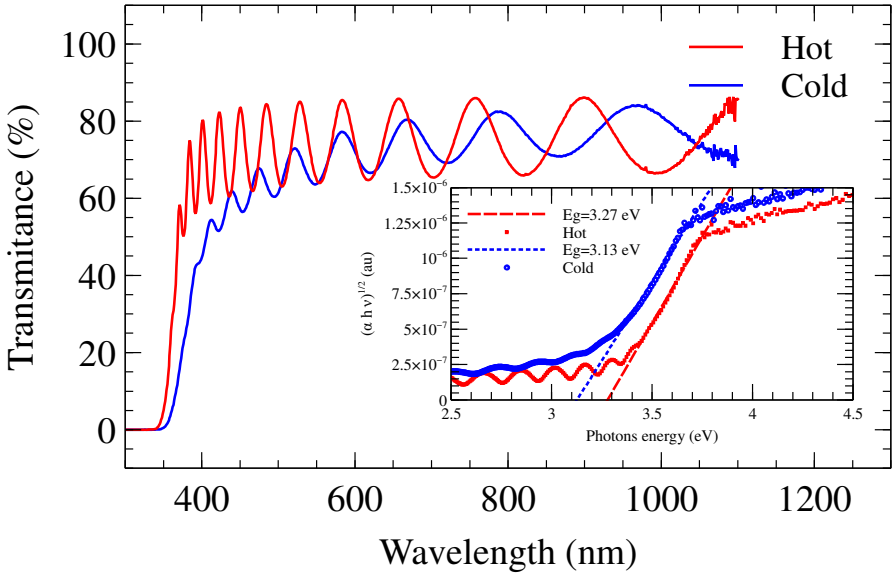

Figure 6: Transmittance curves of TiO_x films grown in cold or hot configuration on sapphire substrates. Inset: Tauc' plot (m=1/2) for both films.

On Figure 6 it is seen that transmission of both films is very similar at wavelengths above 700 nm. The periodicity of the oscillations due to interference phenomenon, is related to the film thicknesses. In the 600-800 nm range, the transmission of films is around 70% for both films, that is similar to the transmission reported in literature for TiO_2 thin films [30]. However, the

transmission differs notably in the vicinity of the absorption edge close to the optical bandgap. The optical bandgap energy of the two films was estimated using the Tauc' plot [31] approach which consists of plotting $(\alpha E)^{1/2}$ versus E (inset in Fig. 6), assuming that anatase TiO_2 is considered as an indirect bandgap material [32]. The optical bandgap E_g values of 3.13 eV and 3.27 eV were obtained for films deposited in cold and hot configurations, respectively. Typical values reported for rutile and anatase films grown by reactive sputtering in Ar/O_2 atmosphere are 3.0 eV and 3.2 eV [33], respectively. It is worth noticing that these bandgap energies taken as reference may vary around these values depending on the experimental growth conditions of TiO_2 compounds that affect the composition (possible oxygen deficiency), the morphology (grain size, surface roughness) and the structural defects in the TiO_2 materials.

For instance, the bandgap values E_g are 3.02-3.05 eV for rutile single crystals and 3.00-3.16 eV for rutile films. For anatase single crystals and anatase films, the values are 3.2 eV and 3.15-3.40 eV, respectively [34]. In addition, the bandgap values determined from the Tauc' plot depend upon the type of the expected optical transitions: very recently, V.V. Shymanovska et al. [35] obtained E_g values of 3.03 and 2.86 eV for anatase thin films considering a direct-allowed and indirect-allowed transitions, respectively, while E_g are 3.23 and 3.13 eV for direct- and indirect- transitions in rutile films. These data show that our values are in good agreement with the results published elsewhere and are related to the formation of anatase- or rutile-based films. The obtained optical bandgap of 3.13 eV for the film grown in cold configuration is consistent with the presence of rutile together with anatase: the bandgap energy of rutile being lower than that of anatase, the E_g value of the film decreases compared to a pure anatase film. In addition, the low value of optical gap obtained in cold configuration (than the one obtained in hot configuration) may also be related to its worst crystallinity since poorly crystallized materials may show localized states which extend into the forbidden band leading to a decrease of the bandgap [36].

Pure anatase structure obtained in hot configuration is not consistent with previous works from Domaradzki et al. [21] who observed a mixture of rutile and anatase in this configuration leading to a bandgap of 3.09 eV±0.03 eV for similar thickness of TiO_2 thin film (800 nm in their work and 930 nm in our case). Our value of bandgap is much closer to the one they obtained for thinner films (415 nm) in hot configuration (3.34 eV±0.06 eV for 415 nm) which shows anatase structure. Such comparison confirms that the crystalline phases and consequently the optical bandgap depend on the film thickness and the configuration.

The film obtained in hot configuration constituted by anatase, exhibits a slightly larger optical bandgap (3.27 eV) than that of reference anatase (3.2 eV). The increase of optical bandgap (i.e.

blue shift) is well described by the Burstein-Moss effect [37] and is related to the conduction band filling due to a higher intrinsic carrier density which limits thermal and optical excitation. Such behaviour, low transparency and high intrinsic carrier density, is classically interpreted as oxygen vacancies in oxide thin films, which lead to donor states in the conduction band. It can be noted that the measurement of oxygen content by RBS in films evidenced a O/Ti ratio around 2, indicating the formation of stoichiometric (or nearly stoichiometric) anatase film. But, considering the low uncertainty on oxygen content determined by RBS (around 5%), it may therefore not be excluded that a slight oxygen deficiency could be at the origin of the small increase of the optical bandgap observed in the case of hot configuration. Yang et al have reported such an increase of the optical bandgap on Al-doped ZnO thin films when a hot configuration is used [38]. They also highlighted that the crystalline quality is enhanced, which indicates reduced defects and grain boundaries. This agrees with our results, since a narrowing of the anatase phase peaks have been detected when turning from cold to hot configuration on this set of samples (see Figure 5).

Conclusion

Structural, morphological and optical properties of TiO_x films deposited by hot Ti target reactive sputtering have been investigated and compared with the classical cold target configuration. Due to the limited power density used in this work (7.4 $W.cm^{-2}$), the reached target temperature remains far from the titanium melting point. As a consequence, the substrate temperature during the growth does not rise a lot in hot target configuration: it was evaluated to be lower than 150°C in cold configuration and around 220°C in hot configuration. Even at temperatures far from the melting point, IR light emitted from a self-heating target influence the growth of a film in reactive sputtering and this confirms first trends observed in [9]. However, in this limited range of temperature, SEM and AFM observations pointed out the furthered role of adatom mobility in hot configuration as compared to cold one, influencing the morphology, the density, the roughness, and the main crystalline orientation of the TiO_x films. This has been found in good agreement with what could be expected from the structure zone model turning from 1c to well-known T zone.

In our experimental conditions, the use of a hot target configuration allows to grow crystallized and singled phase anatase TiO_2 films while the films obtained in classical cold configuration are constituted by a mixture of anatase and rutile with a lowest crystallinity. Consequently, a

better optical transparency in the UV-Vis-nearIR range is observed for hot target MS TiO_2 films and the optical bandgap (3.27 eV) of these films is close to the classical values obtained elsewhere. Reactive MS in Ar/O_2 with self-heating target is an interesting way to produce oxide films with better properties compared with those obtained in classical MS while avoiding heating the substrate.

Acknowledgements

Part of this work was supported by the CERTeM 2020. The first author thanks the "Region Centre Val de Loire" for financial supports during his PhD. The authors thank Thierry SAUVAGE, Olivier WENDLING and Aurelien BELLAMY from the CEMHTI laboratory for RBS measurements on the Pelletron accelerator.

References

[1] S. Sério, M.E. Melo Jorge, M.L. Coutinho, S.V. Hoffmann, P. Limão-Vieira, Y. Nunes, Spectroscopic studies of anatase TiO_2 thin films prepared by DC reactive magnetron sputtering, Chemical Physics Letters. 508 (2011) 71–75. https://doi.org/10.1016/j.cplett.2011.04.002.

[2] A. Amin, D. Köhl, M. Wuttig, The role of energetic ion bombardment during growth of TiO_2 thin films by reactive sputtering, Journal of Physics D: Applied Physics. 43 (2010) 405303. https://doi.org/10.1088/0022-3727/43/40/405303.

[3] A. Vahl, S. Veziroglu, B. Henkel, T. Strunskus, O. Polonskyi, O.C. Aktas, F. Faupel, Pathways to Tailor Photocatalytic Performance of TiO_2 Thin Films Deposited by Reactive Magnetron Sputtering, Materials. 12 (2019) 2840. https://doi.org/10.3390/ma12172840.

[4] V.I. Shapovalov, A.V. Zav'yalov, A.A. Meleshko, Current-voltage characteristics of a magnetron with a hot titanium target in chemically active environments, Surface and Coatings Technology. 417 (2021) 127189. https://doi.org/10.1016/j.surfcoat.2021.127189.

[5] D.P. Aun, M. Houmard, M. Mermoux, L. Latu-Romain, J.-C. Joud, G. Berthomé, V.T.L. Buono, Development of a flexible nanocomposite TiO2 film as a protective coating for bioapplications of superelastic NiTi alloys, Applied Surface Science. 375 (2016) 42–49. https://doi.org/10.1016/j.apsusc.2016.03.064.

[6] C. Euvananont, C. Junin, K. Inpor, P. Limthongkul, C. Thanachayanont, TiO_2 optical coating layers for self-cleaning applications, Ceramics International. 34 (2008) 1067–1071. https://doi.org/10.1016/j.ceramint.2007.09.043.

[7] J. Musil, D. Herman, J. Sícha, Low-temperature sputtering of crystalline TiO_2 films, J. of Vacuum Science & Technology A24 (2006) 521 . https://doi.org/10.1116/1.2187993.
[8] H. Toku, R.S. Pessoa, H.S. Maciel, M. Massi, U.A. Mengui, Influence of process parameters on the growth of pure-phase anatase and rutile TiO2 thin films deposited by low temperature reactive magnetron sputtering, Braz. J. Phys. 40 (2010) 2126-2131 https://doi.org/10.1590/S0103-97332010000300015.
[9] B. Wang, S. Wei, L. Guo, Y. Wang, Y. Liang, B. Xu, F. Pan, A. Tang, X. Chen, Effect of deposition parameters on properties of TiO2 films deposited by reactive magnetron sputtering, Ceramics International. 43 (2017) 10991–10998. https://doi.org/10.1016/j.ceramint.2017.05.139.
[10] D. Rafieian, W. Ogieglo, T. Savenije, R.G.H. Lammertink, Controlled formation of anatase and rutile TiO_2 thin films by reactive magnetron sputtering, AIP Advances. 5 (2015) 097168. https://doi.org/10.1063/1.4931925.
[11] S. Mahieu, P. Ghekiere, D. Depla, R. De Gryse, Biaxial alignment in sputter deposited thin films, Thin Solid Films. 515 (2006) 1229–1249. https://doi.org/10.1016/j.tsf.2006.06.027.
[12] A.V. Kaziev, D.V. Kolodko, A.V. Tumarkin, M.M. Kharkov, V.Yu. Lisenkov, N.S. Sergeev, Comparison of thermal properties of a hot target magnetron operated in DC and long HIPIMS modes, Surface and Coatings Technology. 409 (2021) 126889. https://doi.org/10.1016/j.surfcoat.2021.126889.
[13] V.V. Karzin, A.E. Komlev, K.I. Karapets, N.K. Lebedev, Simulation of heating of the target during high-power impulse magnetron sputtering, Surface and Coatings Technology. 334 (2018) 269–273. https://doi.org/10.1016/j.surfcoat.2017.11.049.
[14] J. Tesař, J. Martan, J. Rezek, On surface temperatures during high power pulsed magnetron sputtering using a hot target, Surface and Coatings Technology. 206 (2011) 1155–1159. https://doi.org/10.1016/j.surfcoat.2011.08.005.
[15] G.A. Bleykher, D.V. Sidelev, V.A. Grudinin, V.P. Krivobokov, M. Bestetti, Surface erosion of hot Cr target and deposition rates of Cr coatings in high power pulsed magnetron sputtering, Surface and Coatings Technology. 354 (2018) 161–168. https://doi.org/10.1016/j.surfcoat.2018.09.030.
[16] V.A. Grudinin, G.A. Bleykher, D.V. Sidelev, V.P. Krivobokov, M. Bestetti, A. Vicenzo, S. Franz, Chromium films deposition by hot target high power pulsed magnetron sputtering: Deposition conditions and film properties, Surface and Coatings Technology. 375 (2019) 352–362. https://doi.org/10.1016/j.surfcoat.2019.07.025.
[17] D.V. Sidelev, G.A. Bleykher, V.P. Krivobokov, Z. Koishybayeva, High-rate magnetron sputtering with hot target, Surface and Coatings Technology. 308 (2016) 168–173. https://doi.org/10.1016/j.surfcoat.2016.06.096.
[18] R. Chodun, M. Dypa, B. Wicher, K. Nowakowska – Langier, S. Okrasa, R. Minikayev, K. Zdunek, The sputtering of titanium magnetron target with increased temperature in reactive atmosphere by gas injection magnetron sputtering technique,

Applied Surface Science. 574 (2022) 151597.
https://doi.org/10.1016/j.apsusc.2021.151597.
[19] A. Billard, D. Mercs, F. Perry, C. Frantz, Influence of the target temperature on a reactive sputtering process, Surface and Coatings Technology. 116–119 (1999) 721–726.
https://doi.org/10.1016/S0257-8972(99)00261-3.
[20] R. Wasielewski, J. Domaradzki, D. Wojcieszak, D. Kaczmarek, A. Borkowska, E.L. Prociow, A. Ciszewski, Surface characterization of TiO2 thin films obtained by high-energy reactive magnetron sputtering, Applied Surface Science. 254 (2008) 4396–4400.
https://doi.org/10.1016/j.apsusc.2008.01.017.
[21] J. Domaradzki, D. Kaczmarek, E.L. Prociow, A. Borkowska, D. Schmeisser, G. Beuckert, Microstructure and optical properties of TiO2 thin films prepared by low pressure hot target reactive magnetron sputtering, Thin Solid Films. 513 (2006) 269–274.
https://doi.org/10.1016/j.tsf.2006.01.049.
[22] R. Graillot-Vuillecot, A.-L. Thomann, T. Lecas, C. Cachoncinlle, E. Millon, A. Caillard, Hot target magnetron sputtering process: Effect of infrared radiation on the deposition of titanium and titanium oxide thin films, Vacuum. 181 (2020) 109734.
https://doi.org/10.1016/j.vacuum.2020.109734.
[23] J. Domaradzki, D. Kaczmarek, A. Borkowska, D. Schmeisser, S. Mueller, R. Wasielewski, A. Ciszewski, D. Wojcieszak, Influence of annealing on the structure and stoichiometry of europium-doped titanium dioxide thin films, Vacuum. 82 (2008) 1007–1012.
https://doi.org/10.1016/j.vacuum.2008.01.021.
[24] H.J. Kim, High mobility Si0.15Ge0.85 growth by using the molten target sputtering (MTS) within heteroepitaxy framework, Sci Rep. 9 (2019) 11555.
https://doi.org/10.1038/s41598-019-47723-2.
[25] R. Brüggemann, P. Reinig, M. Hölling, Thickness dependence of optical scattering and surface roughness in microcrystalline silicon, Thin Solid Films. 427 (2003) 358–361.
https://doi.org/10.1016/S0040-6090(02)01230-0.
[26] I. Petrov, P.B. Barna, L. Hultman, J.E. Greene, Microstructural evolution during film growth, Journal of Vacuum Science & Technology A: Vacuum, Surfaces, and Films. 21 (2003) S117–S128.
https://doi.org/10.1116/1.1601610.
[27] S. Van Steenberge, W.P. Leroy, D. Depla, Influence of oxygen flow and film thickness on the texture and microstructure of sputtered ceria thin films, Thin Solid Films. 553 (2014) 2–6.
https://doi.org/10.1016/j.tsf.2013.11.049.
[28] A. Anders, A structure zone diagram including plasma-based deposition and ion etching, Thin Solid Films. 518 (2010) 4087–4090.
https://doi.org/10.1016/j.tsf.2009.10.145.
[29] J.A. Thornton, D.W. Hoffman, Stress-related effects in thin films, Thin Solid Films. 171 (1989) 5–31.
https://doi.org/10.1016/0040-6090(89)90030-8.

[30] W. Zhang, Y. Li, S. Zhu, F. Wang, Influence of argon flow rate on TiO_2 photocatalyst film deposited by dc reactive magnetron sputtering, Surface and Coatings Technology. 182 (2004) 192–198. https://doi.org/10.1016/j.surfcoat.2003.08.050.
[31] J. Tauc, Absorption edge and internal electric fields in amorphous semiconductors, Materials Research Bulletin. 5 (1970) 721–729. https://doi.org/10.1016/0025- 5408(70)90112-1.
[32] P. Makuła, M. Pacia, W. Macyk, How To Correctly Determine the Band Gap Energy of Modified Semiconductor Photocatalysts Based on UV–Vis Spectra, J. Phys. Chem. Lett. 9 (2018) 6814–6817. https://doi.org/10.1021/acs.jpclett.8b02892.
[33] H. Tang, K. Prasad, R. Sanjinès, P.E. Schmid, F. Lévy, Electrical and optical properties of TiO $_2$ anatase thin films, Journal of Applied Physics. 75 (1994) 2042–2047. https://doi.org/10.1063/1.356306.
[34] K. Möls, L. Aarik, H. Mändar, A. Kasikov, A. Niilisk, R. Rammula, J. Aarik, Influence of phase composition on optical properties of TiO2: Dependence of refractive index and band gap on formation of TiO2-II phase in thin films, Optical Materials. 96 (2019) 109335. https://doi.org/10.1016/j.optmat.2019.109335.
[35] V.V. Shymanovska, T.A. Khalyavka, E.V. Manuilov, T.A. Gavrilko, A. Aho, V.V. Naumov, N.D. Shcherban, Effect of surface doping of TiO_2 powders with Fe ions on the structural, optical and photocatalytic properties of anatase and rutile, Journal of Physics and Chemistry of Solids. 160 (2022) 110308. https://doi.org/10.1016/j.jpcs.2021.110308.
[36] B. Astinchap, K.G. Laelabadi, Effects of substrate temperature and precursor amount on optical properties and microstructure of CVD deposited amorphous TiO_2 thin films, Journal of Physics and Chemistry of Solids. 129 (2019) 217–226. https://doi.org/10.1016/j.jpcs.2019.01.012.
[37] N.F. Mott, Conduction in non-crystalline materials: III. Localized states in a pseudogap and near extremities of conduction and valence bands, Philosophical Magazine. 19 (1969) 835–852. https://doi.org/10.1080/14786436908216338.
[38] W.F. Yang, Z.G. Liu, Z.Y. Wu, M.H. Hong, C.F. Wang, A.Y.S. Lee, H. Gong, Low substrate temperature fabrication of high-performance metal oxide thin-film by magnetron sputtering with target self-heating, Appl. Phys. Lett. 102 (2013) 111901. https://doi.org/10.1063/1.4795763.